ELSEVIER

Intermetallics 10 (2002) 1215–1219

Intermetallics

www.elsevier.com/locate/intermet

Magnetic properties and microstructural characteristics of bulk Nd–Al–Fe–Co glassy alloys

Pan Mingxiang[a,*], Wei Bingchen[b], Xia Lei[a], Wang Weihua[a], Zhao Deqian[a], Zhang Zhi[a], Han Bao Shan[a]

[a]*Institute of Physics, Chinese Academy of Science, Beijing 100080, China*
[b]*National Microgravity Laboratory, Institute of Mechanics, Chinese Academy of Sciences, Beijing 100080, China*

Accepted 21 August 2002

Abstract

Bulk Nd–Al–Fe–Co glassy alloys with diameter up to 5 mm were investigated by magnetic measurements, magnetic force microscopy (MFM) and high resolution electron microscopy (HREM) at room temperature. The results from the measurement of vibrating sample magnetometer show that these samples with compositions $Nd_{65}Al_{10}Fe_{25-x}Co_x$ ($x=0$–10 at.%) and $Nd_{60}Al_{10}Fe_{20}Co_{10}$ display hard magnetic properties with H_C of $\sim$300 kAm^{-1}, M_S of $\sim$10 Am^2 kg^{-1}, and M_r of $\sim$7 Am^2 kg^{-1}. The MFM measurements of the $Nd_{60}Al_{10}Fe_{20}Co_{10}$ bulk metallic glass (BMG) reveal the existence of magnetic domains with a period of about 0.36 μm, and the ordered clusters with the averaged size of about 5 nm was observed by the HREM on the sample. The domain structure or cluster is believed to be associated with the appearance of hard-magnetic properties in this alloy system. The existence of the large-size domains demonstrates that magnetic moment of a great deal of ordered atomic clusters in the BMG has been aligned by exchange-coupling.

Keywords: B. Glasses, metallic

1. Introduction

Nd–Fe-based bulk metallic glass (BMG) alloy is attracting more and more attentions in recent years because of novel magnetic behavior [1–5]. For example, while Nd–Fe and Pr–Fe amorphous alloy ribbons showed hard magnetic properties at low temperatures [6], the $Nd_{60}Fe_{30}Al_{10}$ in bulk forms was found to exhibit a hard magnetism at room temperature, and this property disappears in the full crystallized $Nd_{60}Fe_{30}Al_{10}$ BMG [1,7]. However, this alloy displays soft magnetic property when it is in the form of the melt-spin amorphous ribbons [8]. No other bulk amorphous alloys exhibit this type of hard magnetic property besides Nd–Fe- and Pr–Fe-based alloys. The addition of elements such as Si and/or Al leads to the increase of the glass forming ability and to improvement of the hard magnetic properties [8,9]. The high coercivity of these amorphous alloys is striking because no structural anisotropy exists in the disordered packing solid. It is supposed that the BMG is an ensemble of short-scale ordered magnetic atomic clusters in uniform distribution [8]. These clusters consist of Nd and transition elements and possess large random anisotropy. On the other hand, it is very interesting to study the variation of magnetic property with microstructural features because this is a way to produce function composite [4]. In this paper, we report the magnetic properties and microstructural characteristics of bulk Nd–Al–Fe–Co glassy alloys.

2. Experimental methods

Alloy ingots with compositions of $Nd_{65}Al_{10}Fe_{25-x}Co_x$ ($x=0$–10 at.%) and $Nd_{60}Al_{10}Fe_{20}Co_{10}$ were prepared by arc melting from elemental Nd, Fe, Al, and Co with a purity of 99.9% in a Ti-gettered argon atmosphere. Cylindrical specimens of 3–5 mm in diameter and 50 mm in length were prepared from the ingots by die and

* Corresponding author. Tel.: +86-10-82649198; fax: +86-10-82649531.
E-mail address: panmx@aphy.iphy.ac.cn (P. Mingxiang).

0966-9795/02/$ - see front matter
PII: S0966-9795(02)00147-4

suction casting into a copper mold under argon atmosphere. The details of preparation can be seen in Ref. [3]. The structure of the as-cast cylinder was characterized by X-ray diffraction (XRD). Magnetic measurements were performed using a vibrating sample magnetometer with a maximum applied field of 1592 kA/m. The study of domain structure was carried out by using Digital Instruments NanoScope IIIa D-3000 magnetic force microscopy (MFM). It allows the topographic and magnetic force images to be collected separately and simultaneously in the same area of the sample by using tapping/lift modes. For the mode of dynamic detection, the cantilever is vibrated and its resonant frequency f_0 and phase ϕ will be modulated by the magnetic forces exerted on the tip from the stray field H emerged from the magnetic structures in the sample surface layer when the tip is scanning. In the magnetic force images detected by the phase mode, the dark and bright regions correspond to the attractive and repulsive tip-sample interactions, respectively. In our experiment, the tip used was magnetized upward prior to imaging. Its $f_0 = 80.6$ kHz, and its lift-height during scanning was 30 nm. The samples for MFM study were fresh cut from the same cylinder. After grinding and polishing, they were vacuum annealed at 453 K for 6 h to remove the stress built in the surface layer. The specimen for TEM observation was cut from the processed disks and thinned to the thickness required for electron transparency by using Dual Ion Mill System (Gatan, Model 600CTMP) with a protection of liquid nitrogen cold stage. The TEM observations were carried out with a model JEOL-2010 with an accelerating voltage of 200 kV.

3. Results and discussions

The X-ray diffraction results show amorphous structural characteristic for the as-cast cylinders in all range of compositions. Fig. 1 exhibits hysteresis loops as a function of the Fe and Co contents of the bulk $Nd_{65}Al_{10}Fe_{25-x}Co_x$ amorphous rods at room temperature. From this figure, one can see that these amorphous rods present hard magnetic properties with the coercive forces of 270–3302 kA/m (also see Table 1). This is consistent with Inoue, Ding and Chiriac's result on ternary NdFeAl bulk metallic amorphous [8,10,11]. The substituting Co for Fe can slightly increase the coercive force (H_c) with Co content up to 10 at.%. When the content of Co is higher than 5 at.%, the residual magnetization (M_r) increases from 7.5 Am^2/kg to 8.1 Am^2/kg, and the value is decreased to 6.4 Am^2/kg when the Co content is 10 at.%. The component element substitution is taken as a valid way to improve magnetic properties. However, the substitution of other elements such as Ni, Cu and B for Fe does not improve magnetic properties. The addition of Ni can increase the coercive force but cause a decrease of 25% of the residual magnetization at the same time, and the addition of Cu or B reduces the M_r and H_c.

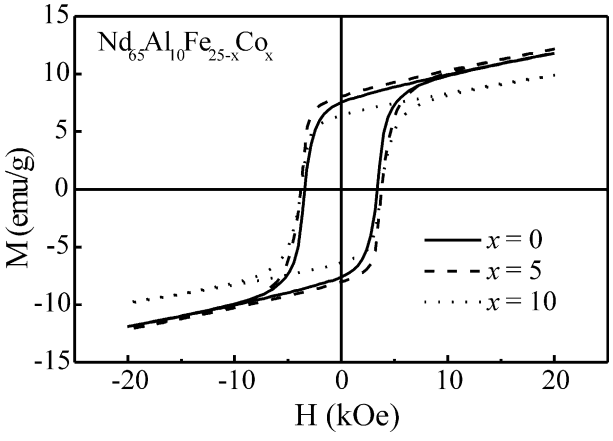

Fig. 1. Hysteresis loops of the as-cast amorphous $Nd_{65}Al_{10}Fe_{25-x}Co_x$ ($x = 0$–10 at.%) alloys with 5 mm diameters at room temperature.

From the results mentioned above, the bulk NdAlFeCo metallic glass is of good hard magnetic properties. In order to study the influence of quenching rate on the hard magnetic properties, we prepared the bulk metallic glasses with different methods. The $Nd_{60}Fe_{30}Al_{10}$ rod with a diameter of 3 mm by die cast method is close to full amorphous (insert in Fig. 2), and the rod from water-quenching is partial amorphous. It is found that

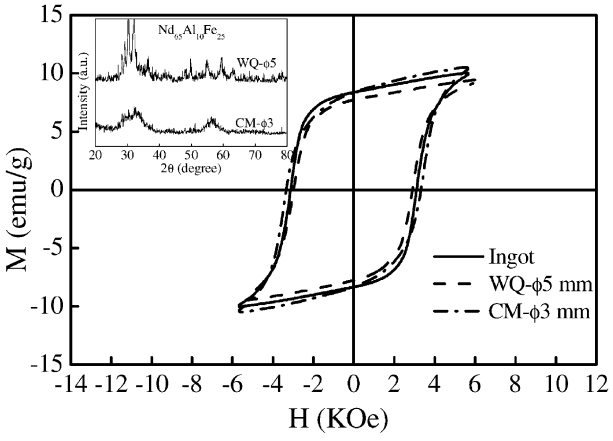

Fig. 2. Hysteresis loops of samples prepared by by water-quenching and copper mould casting. Inset is the XRD diffraction patterns of corresponding samples.

Table 1
Comparison of hard-magentic properties for bulk metallic glass samples with different composition

BMG	M_s (Am^2/kg)	M_r (Am^2/kg)	H_c (kA/m)	T_c (K)
$Nd_{65}Al_{10}Fe_{25}$	11.79	7.53	271.4	446
$Nd_{65}Al_{10}Fe_{20}Co_5$	12.18	8.05	302.4	452
$Nd_{65}Al_{10}Fe_{15}Co_{10}$	9.91	6.38	301.2	466
$Nd_{60}Al_{10}Fe_{20}Co_{10}$	10.82	7.22	326.3	465

the hard magnetic properties do not have obviously relationship with the ratio of amorphous fraction in the alloy. The H_c of amorphous rod with a diameter of 5 mm from die casting is largest (not shown here), and the M_r of ingot is highest among these samples. The results from Inoue and Li et al. also show that the ribbon NdAlFe amorphous is of soft magnetic properties [10,12–15], and the BMG is of hard magnetic properties. The BMG has the more relaxed microstructure due to the much larger sample thickness compared to the ribbon amorphous. The fully relaxed microstructure for the cast bulk amorphous alloys develops owing to the slow cooling in the high temperature range where long-range rearrangements of the constituent atoms can occur easily. This means that the hard magnetic properties of the BMG is due to the existence of a large of magnetic Nd–Fe and/or Nd–Nd or other short-range clusters [6,8]. The strong magnetic exchange coupling between these clusters result in the hard-magnetic properties. The BMG prepared by water quenching has more high relaxed structure than that from copper mould casting, but this does not increase the coercive force of the BMG. This effect indicates a possibility of producing a new type of amorphous alloys with well-controlled cluster microstructure (clustered or nanometer amorphous alloy) [4].

To reveal the hard magnetic mechanism in the as-cast BMG intuitively, the magnetic domain structure in the as-cast BMG is observed by using MFM. Obvious magnetic contrast was exhibited in the magnetic force images. For the as-cast BMG, a typical magnetic force image for 10×10 μm^2 area is shown in Fig. 3. It can be seen that the image is characterized by dark regions adjacent with bright regions in submicron scale and in random distribution. The dark regions present that the magnetization direction in this region is nearly parallel to the upward tip magnetization, and the bright regions for the opposite. This kind of magnetic contrast is similar to the so-called "exchange coupling domains" appeared in the nanocomposite rare-earth-transition metal permanent materials, in which strong exchange-coupling interaction exists between hard and soft magnetic grains [16,17]. The average period (T) of the domain pattern and the average contrast between dark and bright regions were measured by means of section analysis and $T=0.36$ μm.

After annealing at 773 K for 30 min, the sample crystallizes completely, and exhibits paramagnetism as

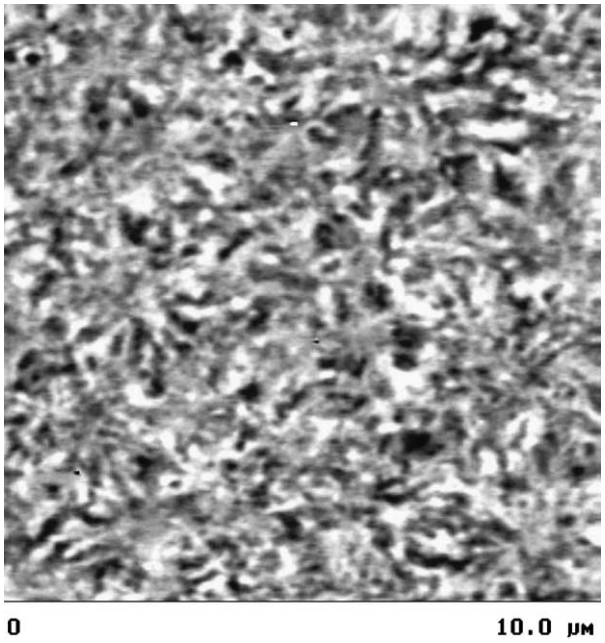

Fig. 3. Magnetic-force image with a scan size 10×10 μm for the as-cast $Nd_{60}Al_{10}Fe_{20}Co_{10}$ BMG.

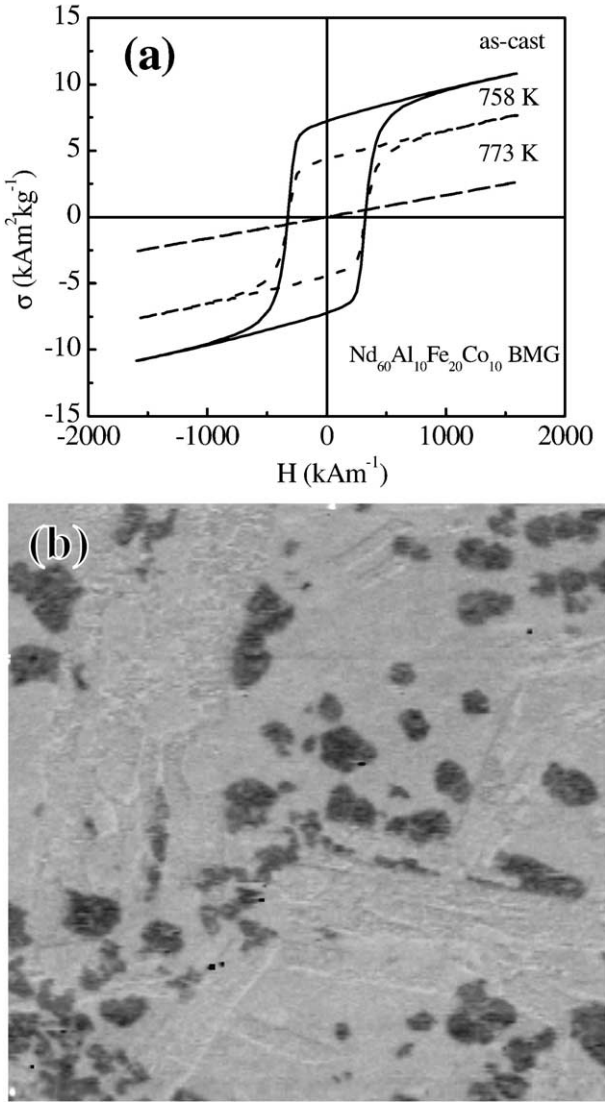

Fig. 4. Dependence hysteresis loop on isothermal annealing temperature for $Nd_{60}Al_{10}Fe_{20}Co_{10}$ BMG (a), and Magnetic force image with a scan size 20 μm×20 μm for the $Nd_{60}Al_{10}Fe_{20}Co_{10}$ BMG (b). Annealing at 773 K for 30 min.

shown in Fig. 4a. Fig. 4b shows its magnetic force image with a scan size of 20×20 μm. It is revealed that the magnetic force image of the fully crystallized sample is much different with that of the as-cast one. No obvious wide distributed magnetic contrast is observed in this figure, except for a small quantity of dark block-like magnetic domains. The magnetic contrast indicates that the magnetic domains are of ferromagnetic crystalline phase. Statistical analysis of the images shows that these ferromagnetic phases have an average size of 0.9 μm.

For the possible existence of the clustered amorphous structure in the BMG, HREM examination is further carried out to show the microstructural characteristic from atomic scale. Fig. 5 presents a HREM image of the as-cast $Nd_{60}Al_{10}Fe_{20}Co_{10}$ sample. There are a large number of ordered cluster regions distributing randomly in the amorphous matrix, and the averaged size of the cluster is about 5 nm. High resolution image shows fringe-like features with a spacing of 0.273 nm in these clusters [18]. These fringe-like clusters only rarely display obvious contrast difference from amorphous matrix. Most of these fringes are parallel and straight as observed in Pd–Si alloy, in contrast to the curved fringes often seen in oxide glasses. The electron diffraction pattern shows the typical amorphous structure in the region containing these clusters as presented in the insert of Fig. 6. It is very surprising that these fringes seem not to represent crystallographic planes because the distances between two adjacent fringes are uniform 0.273 nm in all ordered clusters. This phenomenon is to be studied in future in detail.

According to the cluster model of the Nd–Fe melt-spinning magnetic system, the exchange-coupling interaction among magnetic clusters with random anisotropy could cause the high coercivity of the magnetic system [19,20]. Inoue et al. confirmed the presence of these short-range ordered clusters in Pr–Fe–Al BMG by radial distribution function studies and in Nd–Fe–Al BMG by HREM [8]. In present study, the as-cast BMG exhibits a typical amorphous X-ray diffraction pattern without obvious crystalline reflection peaks. This gives an upper limit of a few nanometers for the cluster size, and is consistent with our HREM result above. However, in the foregoing section the analysis of the magnetic force images of the $Nd_{60}Al_{10}Fe_{20}Co_{10}$ BMG has shown that their magnetic domains are in submicron scale, which is significantly larger than the size of the ordered atomic clusters composed of the Nd–Fe and Nd–Co atoms. We infer that it is the experimental evidence of the existence of strong exchange coupling. It is by the exchange coupling that a great deal of short-scale ordered atomic clusters are aligned to form the large-scale magnetic domains. In other words, the large areas of magnetic contrast are actually a collection of a group of clusters with similar magnetic orientation aligned by exchange coupling. Furthermore, the presence of strong exchange coupling is also confirmed by the significant remanence enhancement of our BMG. Its M_r/M_s value is 0.67, which is obviously greater than 0.5, the value predicted for randomly oriented and non-interacting particles by the Stoner–Wohlfarth theory [17]. Like other researchers' results, no such large-size clusters in melt-spinning amorphous ribbon were revealed by HREM observation [21].

The thermal stability of the hard magnetic properties is examined by isothermal annealing of the BMG samples. Fig. 6 shows the dependence of coercivity H_c, saturation magnetization M_s and remanence M_r on isothermal annealing temperature for the $Nd_{60}Al_{10}Fe_{20}Co_{10}$ BMG. The hard magnetic properties remain almost unchanged in the annealing temperature range from room temperature up to 740 K, and disappear after full crystallization of the BMG above 760 K. The presence of only one magnetic phase in the as-cast

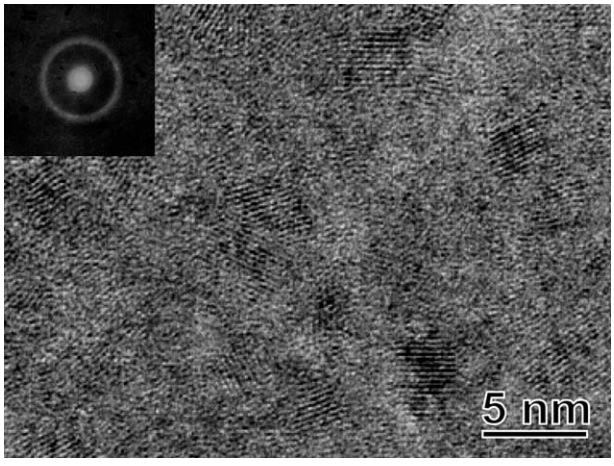

Fig. 5. HREM image of the as-cast $Nd_{60}Al_{10}Fe_{20}Co_{10}$ BMG.

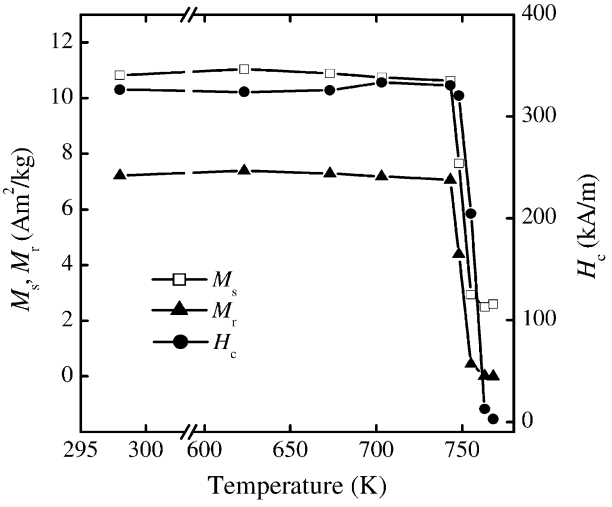

Fig. 6. Dependence of H_c, M_s, and M_r on isothermal annealing temperature for $Nd_{60}Al_{10}Fe_{20}Co_{10}$ alloy (annealing for 30 min).

cylinders was confirmed by the curve of magnetization vs temperature, in which only one magnetic transition appears at Curie temperature of about 470 K before crystallization.

4. Conclusion

The magnetic properties and microstructural characteristic of bulk Nd–Al–Fe–Co glassy alloys were studied by vibrating sample magnetometer, and magnetic force microscopy and high resolution electron microscopy at room temperature. The results reveal $Nd_{65}Al_{10}Fe_{25-x}Co_x$ ($x=0$–10 at.%) and $Nd_{60}Al_{10}Fe_{20}Co_{10}$ exhibit hard-magnetic properties. The presence of exchange coupling interaction between a great deal of fringe-like ordered magnetic atomic clusters in $Nd_{60}Al_{10}Fe_{20}Co_{10}$ BMG is experimentally confirmed by the magnetic force images, and the existence of ordered clusters is revealed by HREM observation. The exchange coupling domains shed light on the appearing of macroscopic hard magnetic properties in the BMG.

Acknowledgements

The authors thank Ms. Shan Xiaoou for the observation in HREM. This work was financially supported by National Natural Science Foundation of China (Grant No.: 50031010, 10174088).

References

[1] Inoue A, Zhang T, Takeuchi A, Zhang W. Mater Trans, JIM 1996;37:636.
[2] Li Y, Ng SC, Lu ZP, Feng YP, Lu K. Philos Mag Lett 1998;78:213.
[3] Wei BC, Zhang Y, Zhuang YX, Zhao DQ, Pan MX, Wang WH, Hu WR. J Appl Phys 2001;89:3529.
[4] Schneider S, Bracchi A, Samwer K. Appl Phys Lett 2002;80:1749.
[5] Chiriac H, Lupu N. J Non-Cryst Solids 2001;287:135.
[6] Croat JJ. J Appl Phys 1982;53:3161.
[7] Wei BC, Wang WH, Pan MX. Phys Rev, B 2001;64:12406.
[8] Inoue A, Takeuchi A. Zhang Tao, Metall Mater Trans A 1998; 29A:1779.
[9] Chiriac H, Lupu N. Mater Sci Eng 2001;A304-A306:727.
[10] Ding J, Li Y, Wang XZ. J Phys D: App Phys 1999;32:713.
[11] Fan GJ, Loser W, Roth S, Eckert J, Schultz L. Appl Phys Lett 1999;75:2984.
[12] Inoue A. Acta Mater 2000;48:279.
[13] Nagayama K, Ino H, Sato N, et al J. Phys Soc Jpn 1990;59:2483.
[14] Skomski R, Coey JMD. Phys Rev B 1993;48:1581.
[15] Schrefl T, Fidler J, Kronmuller H. Phy Rev B 1994;49:6100.
[16] Folks L, Woodward RC. J Magn Magn Mater 1998;190:28.
[17] Al-Khafaji MA, Raiforth WM, Gibbs MRJ, Davies HA, Bishop JEL. J Magn Magn Mater 1998;182:111.
[18] Gaskell PH, Smith DJ, Catto CJD, Cleaver JRA. Nature 1979; 281:465.
[19] Siratori K, Nagayama K, Ino H, Saito N, Nakagawa Y. J Phys Soc Jpn 1990;59:2483.
[20] Taylor RC, McGuire TR, Coey JMD, Gangulee A. J Appl Phys 1978;49:2885.
[21] Wei Bing Chen, Xia Lei et al., unpublished.